DOYLE, P. A., TURNER, P. S. (1968). *Acta Cryst.* A**24**, 390–397.
DRIJVER, J. N. & WOUDE, F. (1977). *Phys. Rev.* **16**, 993–1000.
GEHLEN, P. & COHEN, J. B. (1965). *Phys. Rev.* **139**, A844–A855.
GOMAN'KOV, V. I. (1976). *Fiz. Met. Metalloved.* **42**, no. 2, 415–418.
GRAGG, J. E. JR, BARDHAN, P. & COHEN, J. B. (1971). *Critical Phenomena in Alloys, Magnets and Superconductors*, edited by R. E. MILLS, E. ASCHER & R. I. JAFFEE, pp. 309–337. New York: McGraw-Hill.
GRAGG, J. E. & COHEN, J. B. (1971). *Acta Metall.* **19**, 507–519.
HEILMANN, A. & ZINN, W. (1967). *Z. Metallkd.* **58**, 113–120.
International Tables for X-ray Crystallography (1962). Vol. III. Birmingham: Kynoch Press.
JOSSO, E. (1949). *C. R. Acad. Sci. Paris*, **229**, 594–596.
KOLLIE, T. G. & BROOKS, C. R. (1973). *Phys. Status Solidi*, **19**, 545–553.
KOLLIE, T. G., SCARBROUGH, J. O. & MCELROY, D. L. (1970). *Phys. Rev. B*, **8**, 2831–2839.
OHSHIMA, K. & WATANABE, D. (1976). *Acta Cryst.* A**32**, 883–892.
SCHWARTZ, L. H., MORRISON, L. A. & COHEN, J. B. (1963). *Adv. X-ray Anal.* **7**, 281–301.
SHULL, C. G. & WILKINSON, M. K. (1955). *Phys. Rev.* **97**, 304–310.
SYKES, C. & JONES, F. W. (1937). *Proc. R. Soc. London Ser. A*, **440**, 444.
TURCHI, P., CALVAYRAC, Y. & PLICQUE, F. (1978). *Phys. Status Solidi*, **45**, 229–238.
WAKELIN, R. J. & YATES, E. L. (1953). *Proc. Phys. Soc. London Sect. B*, **66**, 221–223.
WALKER, C. B. & CHIPMAN, D. R. (1970). *Acta Cryst.* A**26**, 447–455.
WILLIAMS, R. O. (1972). ORNL Report 5, Oak Ridge National Laboratory, Tennessee.
WILSON, W. L. & GOULD, R. (1972). *J. Appl. Cryst.* **5**, 125–127.

Acta Cryst. (1980). A**36**, 7–15

A Neutron Diffraction Study of Anharmonic Thermal Vibrations in Cubic $CsPbX_3$

BY M. SAKATA,* J. HARADA,† M. J. COOPER AND K. D. ROUSE

*Materials Physics Division, AERE, Harwell, Oxon., OX*11 0*RA, England*

(*Received* 23 *April* 1979; *accepted* 26 *July* 1979)

Abstract

A neutron diffraction study of cubic $CsPbX_3$ (X = Cl or Br) has been carried out over the temperature ranges 325–623 K for $CsPbCl_3$ and 408–673 K for $CsPbBr_3$. The temperature factors for the perovskite structure were derived following the method of Matsubara [*Prog. Theor. Phys.* (1975), **53**, 1210–1211] which includes the use of cumulant coefficients to characterize anharmonic components for an Einstein model. The potential parameters were then obtained using a numerical integration method to analyse the temperature dependence of the temperature factors. It was found that the anharmonic components in the potential were very large for the Cs and X atoms which undergo displacements on passing through the phase transitions at lower temperatures (321 K for $CsPbCl_3$ and 403 K for $CsPbBr_3$). On the other hand, a harmonic potential is quite adequate to describe the thermal vibration of the Pb atoms, which are not displaced at the phase transitions. Thus, the existence of the anharmonicity in the cubic phase seems to be anticipating the atomic displacement through the successive phase transitions for these substances. In addition to this anharmonicity, the temperature factors of the X atoms parallel to the (100) plane show an anomalous behaviour near the cubic to tetragonal phase-transition temperature, which should be connected with the softening of phonon mode at this phase transition.

1. Introduction

Cesium lead chloride, $CsPbCl_3$, and cesium lead bromide, $CsPbBr_3$, have a cubic perovskite structure at high temperature and show similar successive structural phase transitions from the viewpoint of atomic displacements through the phase transitions; that is, the first phase transition from the high-temperature side is due to the condensation of the M_3 mode, in which atomic displacement is allowed only for X (X = Cl, Br) atoms and others are due to the condensation of the Z_9‡

* On leave from Nagoya University, Nagoya, Japan.
† Applied Physics, Nagoya University, Nagoya, Japan.

‡ This notation is following the representation given by Olbrychski (1963).

0567-7394/80/010007-09$01.00

(R_{25}-like) mode, in which displacement of Cs and X atoms is allowed (*e.g.* Hirotsu, 1971; Ohta, Harada & Hirotsu, 1973; Fujii, Hoshino, Yamada & Shirane, 1974; Hirotsu, Harada, Iizumi & Gesi, 1974). In previous work on cubic $CsPbCl_3$, two of the authors (MS and JH) and others (Harada, Sakata, Hoshino & Hirotsu, 1976) have found no indication of several potential minima, as suggested by Møller (1959), but found that the perovskite model with anisotropic thermal vibrations was quite adequate to describe the thermal behaviour of this substance. They have, however, pointed out that the temperature parameters B_{11} (Cs) and B_{11} (Cl) are extremely large, while the other temperature parameters, B_{11} (Pb) and B_{33} (Cl), are quite normal and strongly suggest the importance of considering anharmonicity for such large temperature parameters, which should play an important role through the phase transitions. Similar anomalies in the temperature parameters B_{11} (Cs) and B_{11} (Br) were found in $CsPbBr_3$ (Sakata, Nishiwaki & Harada, 1979).

In the analysis it has also been found that the generalized Debye–Waller factor expressions including anharmonicity for ABX_3-type structures given by Nishiwaki, Sakata & Harada (1976) are not suitable as yet for the anomalously large temperature parameters B_{11} (Cs) and B_{11} (Br). This fact indicates that the expressions for various average quantities in the power of the anharmonic potential coefficients are not valid for deriving the generalized Debye–Waller factors due to their unbounded nature, as pointed out by Matsubara (1975*b*). In order to investigate the characteristic anharmonicity in such large temperature parameters, structure analysis of cubic $CsPbX_3$ (X = Cl and Br) was carried out by neutron diffraction at some temperatures. The temperature dependence of the temperature parameters was analysed by a numerical integration method for the mean-square atomic displacement on the basis of an anharmonic potential. It was found that this procedure was successful for obtaining anharmonic potential parameters with reasonable accuracy but there exist two potential models for the halogen atoms, both of which describe very well the experimental data.

In this paper we present a numerical integration method to analyse the temperature dependence of the temperature parameters and to obtain the potential parameters including anharmonicity in the Einstein model. The thermal properties of the constituent atoms obtained in these substances are discussed in connection with their structural phase transitions.

2. Temperature factor

The temperature factor expressions proposed by Willis (1969) and Dawson (1967) enable us to investigate the third- and fourth-order anharmonicity. Their methods, based upon the classical Einstein oscillator model, however, adopted a serial expansion approximation in which it was assumed that the contribution of the anharmonicity in the temperature factor was much less than the harmonic contribution. As a result of this approximation, their equations are less satisfactory when there is more significant anharmonic vibration. In an extreme case, their equations could even be inadequate. In addition, the final equation includes a singular point if the isotropic fourth-order anharmonicity is considered. To avoid this deficiency, the generalized temperature factor within the limitation of the classical Einstein oscillator model is derived following Matsubara's (1975*a*,*b*) method.

If the classical Einstein oscillator model is assumed, the generalized temperature factor may be expressed as the exponent of the cumulant expansion by definition,

$$\langle \exp(i\mathbf{Q}\mathbf{u}_j)\rangle = \exp\left[\sum_{n=1}^{\infty}\frac{1}{n!}\langle(i\mathbf{Q}\mathbf{u}_j)^n\rangle_c\right], \qquad (1)$$

where $\mathbf{Q}$ is the scattering vector, $\mathbf{u}_j$ the displacement of the jth atom by thermal vibrations and c means the cumulants. General treatment of (1) leads to the results of Johnson (1970). In his method, however, the physical meaning of each coefficient is not always clear. In this paper, only the temperature factors of atoms in the perovskite structure will be considered. A wider consideration of the temperature factor following the present method will be given in a separate paper.

From now on, it would be better to consider the temperature factors for the Cs and Pb atoms and that for the X atoms separately, because of the different symmetry of these atoms' sites.

(i) *Temperature factors for* Cs *and* Pb *atoms*

If a spherical potential is adopted, the appropriate potential for the atoms following Willis (1969) is

$$V(u) = V_0 + \frac{\alpha}{2}u^2 + \gamma u^4, \qquad (2)$$

where α and γ are isotropic potential coefficients. For this potential, the temperature factor is written as

$$\langle \exp(i\mathbf{Q}\mathbf{u})\rangle = \exp[-\tfrac{1}{3}Q_2\langle u^2\rangle] \times (\text{higher cumulants}). \qquad (3)$$

The second cumulant term is rewritten in the more convenient form

$$\exp[-\tfrac{1}{3}Q_2\langle u^2\rangle] = \exp[-B(\sin\theta/\lambda)^2], \qquad (4)$$

where

$$B = \tfrac{8}{3}\pi^2\langle u^2\rangle = \tfrac{8}{3}\pi^2\frac{\int_0^\infty u^4\exp(-V/k_BT)\,du}{\int_0^\infty u^2\exp(-V/k_BT)\,du}, \qquad (5)$$

where k_B is the Boltzman constant and T the temperature. The right-hand side of (4) is in exactly the same form as the ordinary isotropic temperature factor. The anharmonicity is taken into account using an anharmonic potential, *e.g.* (2), in (5). Clearly, these equations become exactly the same as the ordinary harmonic treatment when $\gamma = 0$, *i.e.*

$$\langle u^2 \rangle = 3k_B T/\alpha. \tag{6}$$

(ii) *Temperature factor for the X atoms*

The temperature factor for the X atoms can also be obtained by the same procedures as in (i). Considering the anisotropy of the site, the relevant potential is written

$$V(\mathbf{u}) = V_0 + V_{\parallel} + V_{\perp}, \tag{7}$$

where the suffixes $\parallel$ and $\perp$ represent directions parallel and perpendiculr to the xy plane, respectively.

$$V_{\parallel} = \frac{\alpha}{2} u_{\parallel}^2 + \gamma u_{\parallel}^4,$$

$$V_{\perp} = \frac{\alpha'}{2} u_{\perp}^2 + \gamma' u_{\perp}^4, \tag{8}$$

$$u_{\parallel}^2 = u_1^2 + u_2^2,$$

$$u_{\perp}^2 = u_3^2. \tag{9}$$

For this potential, the temperature factor is expressed by

$$\langle \exp(i\mathbf{Qu}) \rangle = \exp(-\tfrac{1}{2}Q_{\parallel}^2 \langle u_{\parallel}^2 \rangle - Q_{\perp}^2 \langle u_{\perp}^2 \rangle) \times (\text{higher cumulants}), \tag{10}$$

where

$$Q_{\parallel}^2 = Q_1^2 + Q_2^2,$$

$$Q_{\perp}^2 = Q_3^2. \tag{11}$$

Finally, the second cumulant term is expressed as

$$\exp(-\tfrac{1}{2}Q_{\parallel}^2 \langle u_{\parallel}^2 \rangle - Q_{\perp}^2 \langle u_{\perp}^2 \rangle) = \exp[-(B_{11}/4a^2)(h^2 + k^2) - (B_{33}/4a^2) l^2], \tag{12}$$

where

$$B_{11} = 4\pi^2 \langle u_{\parallel}^2 \rangle = 4\pi^2 \frac{\int u_{\parallel}^3 \exp(-V_{\parallel}/k_B T)\, du_{\parallel}}{\int u_{\parallel} \exp(-V_{\parallel}/k_B T)\, du_{\parallel}}, \tag{13}$$

$$B_{33} = 8\pi^2 \langle u_{\perp}^2 \rangle = 8\pi^2 \frac{\int u_{\perp}^2 \exp(-V_{\perp}/k_B T)\, du_{\perp}}{\int \exp(-V_{\perp}/k_B T)\, du_{\perp}}, \tag{14}$$

and a is the lattice constant. The right-hand side of (12) is in exactly the same form as the conventional harmonic anisotropic temperature factor and the anharmonicity effect on the B values is given in (13) and (14). If the fourth-order anharmonic term in the potential can be ignored, these equations also become exactly the same as the traditional harmonic temperature factors, *i.e.*

$$\langle u_{\parallel}^2 \rangle = 2k_B T/\alpha, \tag{15}$$

$$\langle u^2 \rangle = k_B T/\alpha'. \tag{16}$$

According to the present derivations of B values, the final equations show that harmonic and anharmonic potential coefficients can be determined separately from the temperature dependence of the B value without knowing higher cumulants effects.

3. Experimental

The single-crystal specimens of $CsPbCl_3$ and $CsPbBr_3$ used in this study each had spherical shape with diameters 7 and 5 mm, respectively.

An electric lamp-shaped furnace was used in this study with double-wall heat isolation. The temperature was controlled by a SCR temperature controller and kept within 0·5 K even at the highest temperature, 673 K. The first transition temperatures from the high-temperature side, which are from cubic to tetragonal transitions for both substances, were confirmed by the observation of the appearance of $\frac{1}{2}$ 310 superstructure reflexions. In order to obtain the temperature dependence of the B values of each atom: (1) for $CsPbCl_3$, 49 independent integrated intensities of Bragg reflexions were measured at the following nine temperatures: 325, 328, 333, 373, 423, 473, 523, 573 and 623 K, from just above the cubic–tetragonal transition temperature; (2) for $CsPbBr_3$, 33 intensities, apart from a few exceptions, at eight temperatures: 408, 413, 423, 448, 473, 523, 573 and 673 K. In the case of $CsPbCl_3$, all reflexions of which the sum of the square of indices is less than 42 ($h^2 + k^2 + l^2 \leq 42$) were measured at any temperature. All measurements were carried out on a four-circle neutron diffractometer at AERE Harwell.

4. Data analysis

Data analysis was carried out in two steps. In the first step, integrated Bragg intensity data sets were analysed refining the B value of each atom using the Harwell *TAILS* computer program in which the required possible corrections for extinction, TDS (thermal diffuse scattering) and absorption can be made. In the second step, the potential parameters, α and γ, for each atom were determined using a least-squares refinement in which the single integration of (5), (13) or (14) was carried out by a numerical method.

The temperature factors determined in the first step were treated as the data to determine the potential parameters. However, it is not necessary to divide the analysis into two steps, since the potential parameters could be determined from the Bragg intensities data directly.

(i) *Analysis by TAILS*

In the *TAILS* program, the calculated intensity is given by

$$I_c = sA_\mu(y + \alpha)|F_c|^2 \operatorname{cosec} 2\theta, \qquad (17)$$

where s is the scale factor, A_μ is the absorption factor, y the extinction factor, α the TDS factor and F_c the calculated structure factor. Since there are no significant differences between the values of the temperature factors obtained using the Cooper & Rouse (1970) theory and the Becker & Coppens (1974*a*,*b*) theory for extinction (Sakata, Cooper, Rouse & Willis, 1978), it is not a serious problem which theory should be used. In this work, the Cooper–Rouse formalism was used. The details of *TAILS* can be found elsewhere (*e.g.* Cooper & Rouse, 1971).

In the final stage of this analysis, the fourth cumulant terms which are represented as $\exp[-h_i h_j h_k h_l D_{ijkl}]$, were considered as well as the effective domain radius r^* in the extinction correction. The final results in this analysis are given in Table 1 for $CsPbCl_3$ and Table 2 for $CsPbBr_3$.* In the tables of experimental data, the observed and calculated intensities are listed together with the standard deviations of the observed intensities based on counting statistics and the values of the extinction and TDS factors for all reflexions observed. In cases for which the counting statistics are better than 1% of the observed intensity, this value was adopted as a standard deviation.

* Lists of structure factors for $CsPbCl_3$ and $CsPbBr_3$ have been deposited with the British Library Lending Division as Supplementary Publication No. SUP 34850 (6 pp.). Copies may be obtained through The Executive Secretary, International Union of Crystallography, 5 Abbey Square, Chester CH1 2HU, England.

The values of the effective domain radius for the different temperatures are in excellent agreement with one another in both cases, confirming the self-consistency of the analysis, although the value of the effective domain radius at a given temperature is not well defined for $CsPbBr_3$ because very few reflexions are affected significantly by extinction in this crystal.

An attempt was made to determine all the fourth cumulant coefficients except for those of the Pb atoms which could not reasonably be expected to be significant, judging from the much smaller B value. Nevertheless, these coefficients could not be well determined except for the anisotropic fourth cumulants D_{1122}(Cl) in $CsPbCl_3$. This fact shows that the other fourth cumulant terms are not significant enough to be determined, giving a large standard deviation of the coefficients, often larger than the coefficient value itself. In addition, there is a strong correlation between second and fourth cumulant coefficients of the same atom. For this reason, the analysis including the fourth-order cumulants gives a worse reliability index for most cases. So, even in the case when the standard deviation is smaller than the coefficient value, we conclude that the fourth cumulant term is not significant because of a worse reliability index. It might be possible to determine the fourth cumulant coefficients from measurements of very high Q reflexions using very short wavelength incident neutrons. It is, however, not our present purpose and it is concluded that the fourth cumulant terms of the temperature factor except for D_{1122}(Cl) can be ignored without significant errors in the present case.

The obtained B values are plotted against the temperature in Fig. 1 for $CsPbCl_3$ and Fig. 2 for $CsPbBr_3$. The calculated B values from the harmonic

Table 1. *Results of the least-squares refinement of* $CsPbCl_3$ *using the TAILS program*

T(K)	325	326	333	373	423	473	523	573	623
B(Cs) (Å^2)	6·17 ± 0·09	6·23 ± 0·10	6·27 ± 0·10	6·88 ± 0·09	7·55 ± 0·10	8·13 ± 0·08	8·89 ± 0·08	9·65 ± 0·13	10·1 ± 0·11
B(Pb)	1·98 ± 0·04	1·98 ± 0·04	2·02 ± 0·04	2·27 ± 0·03	2·52 ± 0·04	2·73 ± 0·03	3·08 ± 0·03	3·36 ± 0·04	3·67 ± 0·03
B_{11}(Cl)	14·6 ± 0·17	14·7 ± 0·18	14·7 ± 0·16	14·6 ± 0·14	14·6 ± 0·13	14·9 ± 0·12	15·3 ± 0·11	15·8 ± 0·14	16·3 ± 0·12
B_{33}(Cl)	1·96 ± 0·04	1·97 ± 0·05	1·99 ± 0·05	2·20 ± 0·04	2·54 + 0·04	2·79 ± 0·03	3·06 ± 0·04	3·39 ± 0·04	3·68 ± 0·03
r^* × 10^6 (mm)	0·88 ± 0·11	0·92 ± 0·13	0·89 ± 0·12	0·89 ± 0·11	0·98 ± 0·11	0·79 ± 0·09	0·87 ± 0·07	0·86 ± 0·11	0·92 ± 0·09
D_{1122}(Cl)†	−11·9 ± 2·0	−12·3 ± 2·1	−11·0 ± 2·0	−10·2 ± 1·8	−10·2 ± 1·6	−9·1 ± 1·5	−8·2 ± 1·3	−8·3 ± 1·7	−9·0 ± 1·4
R (%)	2·26	1·79	1·80	1·80	1·26	1·50	1·01	1·11	0·99
wR	4·21	4·54	4·18	4·16	4·04	3·29	3·10	3·57	1·47

† Fourth cumulant coefficient.

Table 2. *Results of the least-squares refinement of* $CsPbBr_3$ *using the TAILS program*

T(K)	408	413	423	448	473	523	573	673
B(Cs) (Å^2)	9·83 ± 0·26	9·90 ± 0·26	10·0 ± 0·22	10·4 ± 0·19	10·6 ± 0·29	11·3 ± 0·28	12·0 ± 0·34	13·5 ± 0·36
B(Pb)	2·96 ± 0·10	2·95 ± 0·10	2·98 ± 0·08	3·16 ± 0·06	3·34 ± 0·10	3·72 ± 0·10	4·10 ± 0·11	4·87 ± 0·12
B_{11}(Br)	18·6 ± 0·28	18·5 ± 0·33	18·0 ± 0·24	18·0 ± 0·18	18·0 ± 0·29	18·4 ± 0·29	18·9 ± 0·34	19·8 ± 0·33
B_{33}(Br)	2·03 ± 0·19	2·13 ± 0·20	2·14 ± 0·17	1·94 ± 0·14	2·01 ± 0·20	2·23 ± 0·21	2·58 ± 0·23	3·44 ± 0·23
r^* × 10^6 (mm)†	0·66 ± 0·40	0·67 ± 0·32	0·66 ± 0·29	0·66 ± 0·20	0·60 ± 0·33	0·65 ± 0·32	0·74 ± 0·30	0·69 ± 0·30
R (%)	3·34	3·68	2·74	2·28	2·95	2·89	2·69	2·69
wR	4·71	5·19	3·99	3·26	4·77	5·13	5·46	5·13

† Effective domain radius for extinction correction.

approximation are shown by a straight dashed line in the figures. The normalizations between observation and calculation were done at 333 K for B(Cs), 373 K for B(Pb) and B_{33}(Cl), 473 K for B_{11}(Cl) in $CsPbCl_3$ and 423 K for B(Cs) and B(Pb), 473 K for B_{11}(Br) and B_{33}(Br) in $CsPbBr_3$. At a glance, it can be seen from the figures that the harmonic approximation is not always adequate to explain the B values obtained by the analysis. In order to interpret these discrepancies between observed and calculated temperature factors by the harmonic approximation, a further analysis of B values has been carried out considering anharmonicity.

(ii) *Analysis of B values*

The B values were analysed by (5), (13) or (14) using another least-squares program and the potential parameters α and γ were refined. In the analyses of B_{11}(Cl), B_{11}(Br) and B_{33}(Br), only four B values at higher temperatures were used. The reason is that these B values show rather anomalous behaviour near the phase transition and the present temperature factor expression does not cover these anomalies. These, therefore, have to be treated separately and will be discussed qualitatively later. In all other cases, all the B values obtained were used in the analyses.

The numerical integrations in (5), (13) and (14) were checked by calculating the harmonic case where the integrations can be solved analytically and the exact answers are known. If the integral range b which replaces the infinite range in the numerical calculation is big enough, say 2 Å, the numerical calculation gives exactly the same value as the correct answer. In the actual calculations, the integral ranges were always checked by confirming the convergence of B values. As an example of this, the convergence of B(Cs) in $CsPbCl_3$ at various temperatures is shown in Fig. 3 where $\alpha = 0{\cdot}419 \times 10^{-19}$ J Å^{-2} and $\gamma = 0{\cdot}109 \times 10^{-19}$ J Å^{-4}. As long as a closed potential is used, it is no problem to determine the integral range and to carry out the integrals numerically.

The final results of this refinement are given in Table 3. All the analyses give very low-weighted reliability indices wR. For the refinement of B_{33}(Br), sixth-order anharmonicity was taken into account to make the potential close, that is, the following potential was used instead of $V_\perp$ in (8),

$$V_\perp = \frac{\alpha'}{2} u_\perp^2 + \gamma' u_\perp^4 + \eta u_\perp^6. \qquad (18)$$

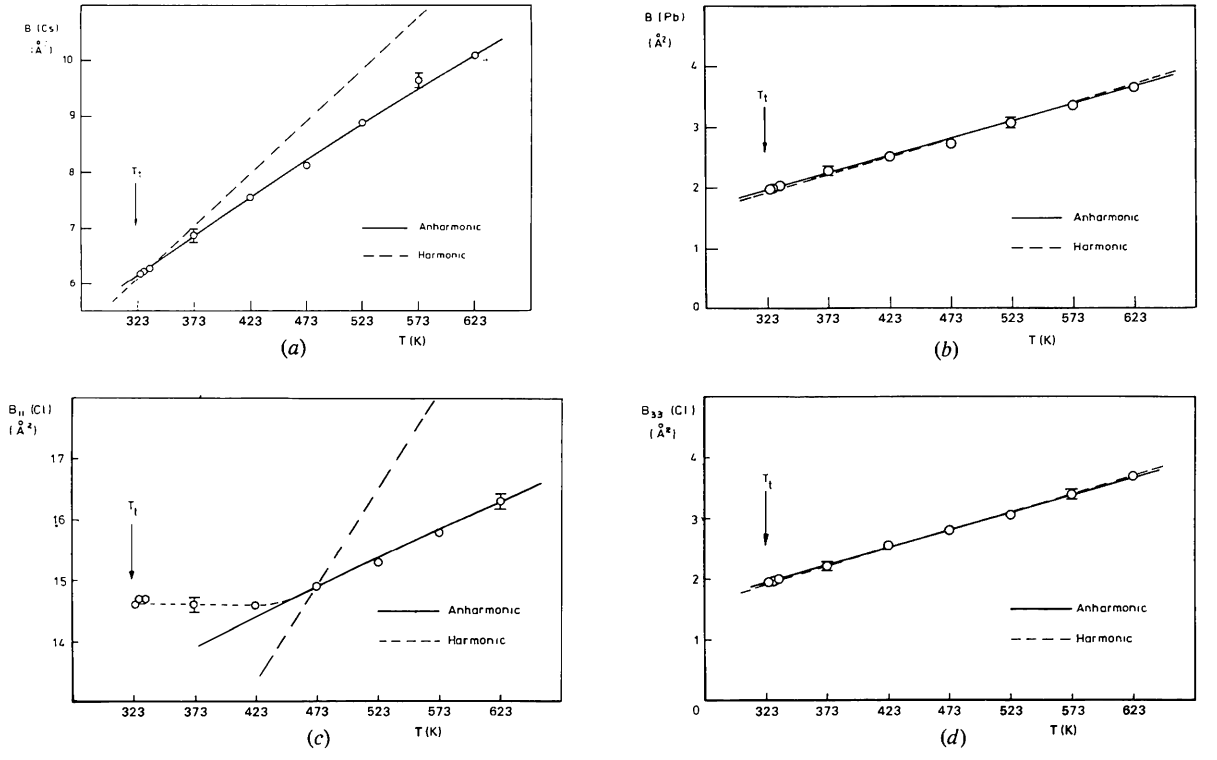

Fig. 1. (*a*) The temperature dependence of B values for Cs atoms in $CsPbCl_3$. The open circles are refined values, solid line is the calculated values using the anharmonic potential in Table 3. The dashed line is calculated values using a harmonic potential. It represents the cubic to tetragonal phase-transition temperature. (*b*) The temperature dependence of B values for Pb atoms in $CsPbCl_3$. (*c*) The temperature dependence of B values parallel to (100) plane for Cl atoms in $CsPbCl_3$. The dotted line near T_c is the guide-of-eye line. (*d*) The temperature dependence of B values perpendicular to (100) plane for Cl atoms in $CsPbCl_3$.

From the table it is very obvious that the harmonic potential is perfectly adequate for the Pb atom in $CsPbBr_3$. For the potentials of V(Pb) and $V_\perp$(Cl) in $CsPbCl_3$ it is not easy to visualize the significance of the anharmonicity, although the fourth-order anharmonic coefficients are well determined. So both harmonic and anharmonic potentials of Pb atoms are shown in Fig. 4. It is very clear from the figures that the anharmonicity of these potentials is not significant. For example, the contribution of anharmonicity in these potentials is less than 3% at the position of the root-mean-square displacement at 623 K, the highest temperature studied. In the figure, the range of measurement is equivalent to the energy at the root-mean-square displacement of the harmonic potential, that is, $(3/2)k_B T$.

The $V_\parallel$(Cl) and $V_\parallel$(Br) potentials are not single minimum potentials, as seen in Fig. 5(*a*) and (*b*) in dotted lines. It should be noticed that the potential barrier between the minima is much smaller than the mean energy of thermal vibration $(3/2)k_B T$. It would be, therefore, reasonable to expect the existence of another possible potential which can also explain the tem-

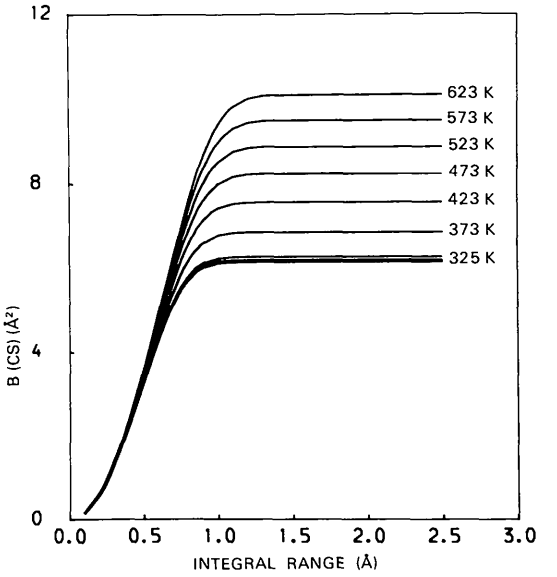

Fig. 3. The convergence of the numerical integral in (5). The B values are plotted against integral range.

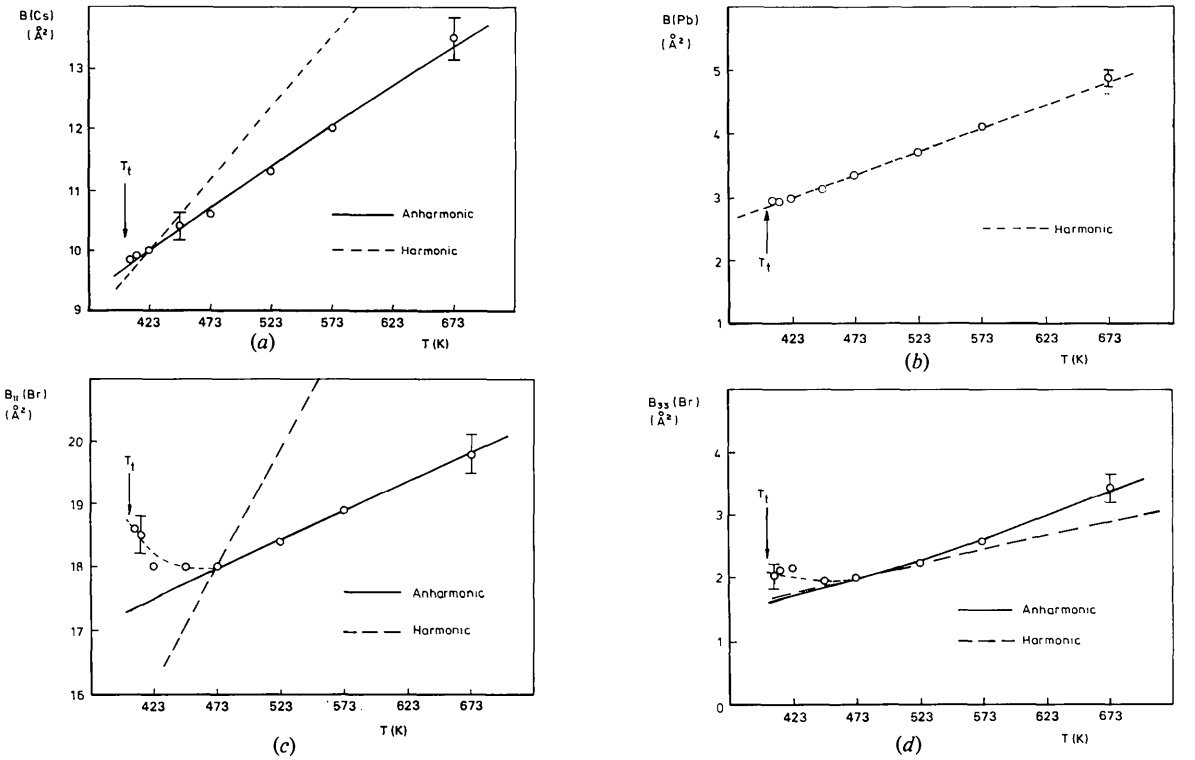

Fig. 2. (*a*) The temperature dependence of B values for Cs atoms in $CsPbBr_3$. The open circles are refined values, solid line is calculated values using the anharmonic potential in Fig. 5. The dashed line is calculated values using a harmonic potential. It represents the cubic to tetragonal phase-transition temperature. (*b*) The temperature dependence of B values for Pb atoms in $CsPbBr_3$. The best fit potential is harmonic. (*c*) The temperature dependence of B values parallel to (100) plane for Br atoms in $CsPbBr_3$. The dotted line near T_t is the guide-of-eye line. (*d*) The temperature dependence of B values perpendicular to (100) plane for Br atoms in $CsPbBr_3$. The dotted line near T_t is the guide-of-eye line.

perature dependence of the observed B_{11}(Cl) and B_{11}(Br). In order to investigate another possible potential, higher-order anharmonicities were considered and it was found that the following simple spherical potentials can also explain the observed B values;

$$V_{\parallel} = \eta u_{\parallel}^6 \text{ for Cl},$$
$$V_{\parallel} = \chi u_{\parallel}^7 \text{ for Br}. \qquad (19)$$

Table 3. *One-particle potential parameters determined by least-squares analysis*

		$CsPbCl_3$	$CsPbBr_3$
Cs:	α	0·419 (1)	0·181 (7)
	γ	0·109 (1)	0·128 (35)
	wR	0·73%	0·77%
Pb:	α	1·742 (2)	1·536 (3)
	γ	0·138 (23)	0·000 (3)
	wR	1·26%	1·08%
X_{11}	α	−0·300 (1)	−0·358 (10)
	γ	0·300 (1)	0·256 (5)
	wR	0·32%	0·19%
$X_{\perp}$	α'	1·784 (1)	3·024 (16)
	γ'	0·128 (27)	−1·222 (22)
	η'	–	0·319 (5)
	wR	0·68%	1·44%
X_{11}	α	–	–
	γ	–	–
	η	0·159 (1)	–
	χ	–	0·088 (1)
	wR	0·28%	0·27%

Units: α (10^{-19} J Å^{-2}), γ(10^{-19} J Å^{-4}), η(10^{-19} J Å^{-6}), χ(10^{-19} J Å^{-7}).

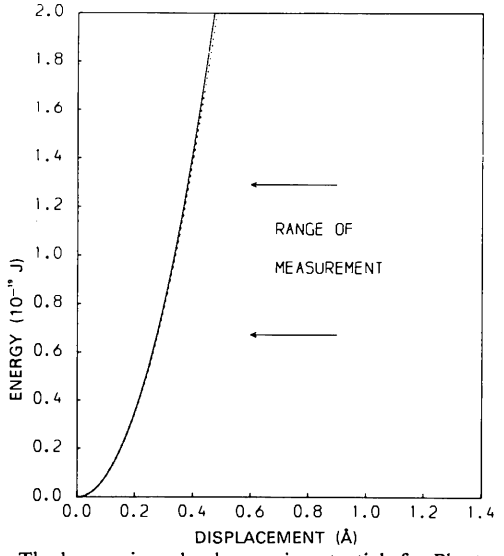

Fig. 4. The harmonic and anharmonic potentials for Pb atoms. As the range of measurement, $(3/2)k_B T$ is used. This energy corresponds to the energy when the particle is displaced at the root-mean-square displacement in a one-particle harmonic potential.

The results of this analysis are also given in Table 3 (bottom row) and the potentials are drawn in Fig. 5 in full lines. From the wR values, it is not possible to conclude which potential is more appropriate, although the shape of the bottom of the potential is very different.

These two kinds of potentials give the same structure factors for all the reflexions so that there would be no way to distinguish these potentials even from Fourier analysis.

5. Fourier analysis

As shown in the least-squares analysis, the fourth-order cumulant coefficient D_{1122} was refined for the Cl atom

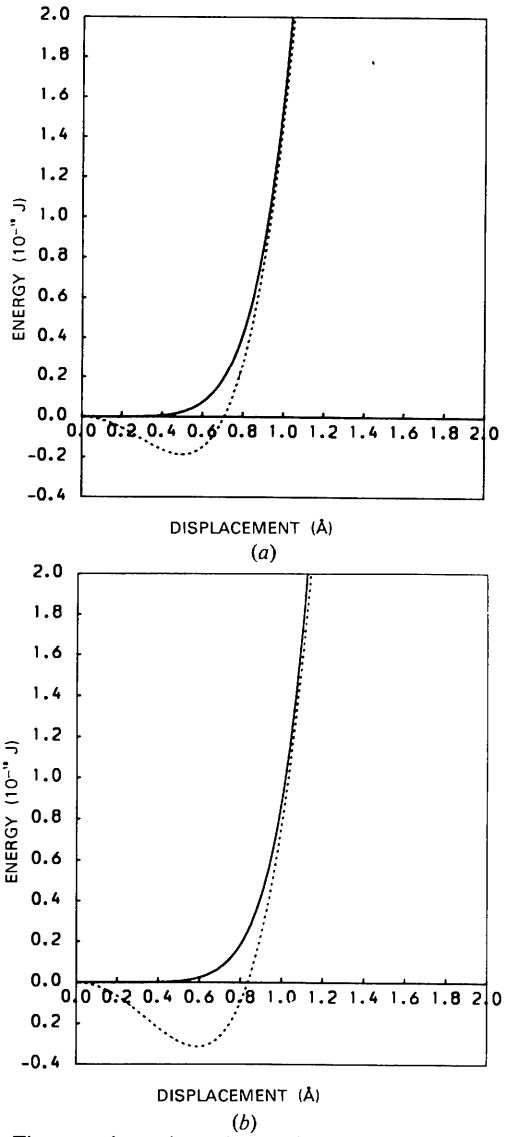

Fig. 5. The two alternative anharmonic potentials for Cl and Br atoms in the direction parallel to (100) plane.

in $CsPbCl_3$, although its standard deviations are rather large compared with other parameters in Table 1. This fact indicates that there exists anisotropic thermal vibrations of the Cl atom in the (100) plane. In order to confirm such anisotropy in the thermal vibration, three-dimensional Fourier and difference Fourier syntheses of $CsPbCl_3$ were carried out at $Z = 0{\cdot}0$ and $0{\cdot}5$ sections for all the temperatures studied. The contour maps of the Fourier syntheses at $Z = 0{\cdot}0$ and $0{\cdot}5$ at 325 K where the thermal vibration is the smallest, are given in Fig. 6(*a*) and (*b*). The resolution of the Fourier synthesis, r, which is $0{\cdot}093a_0$ at all temperatures, is very slightly better than the previous work, $r = 0{\cdot}095a_0$ (Harada, Sakata, Hoshino & Hirotsu, 1976). The resolution is also better than the root-mean-square displacement, $\langle u^2\rangle^{1/2}$ of Cl atoms parallel to the (100) plane. There is no inherent difference between the two results; there is no indication of the existence of a hump among the potential minima for the Cl atoms, which is larger than $(3/2)k_BT$. It is, therefore, concluded that the $V_{\parallel}$(Cl) [and probably $V_{\parallel}$(Br)] potentials are very anharmonic ones with a single minimum. This result contrasts with the same kind of analysis for α-AgI by Cava, Reidinger & Wuensch (1977) in which the disordering of Ag ions was clearly shown on a Fourier synthesis.

In the difference Fourier synthesis, the contributions of the second cumulant term in the temperature factor are subtracted from the observed intensity data for all kinds of atoms. The difference Fourier maps at $Z = 0{\cdot}0$ are shown at two temperatures, 328 and 573 K, in Figs. 7(*a*) and (*b*), respectively. The four small peaks found around the equilibrium positions of Cl atoms indicate clearly the existence of the anisotropic fourth cumulant

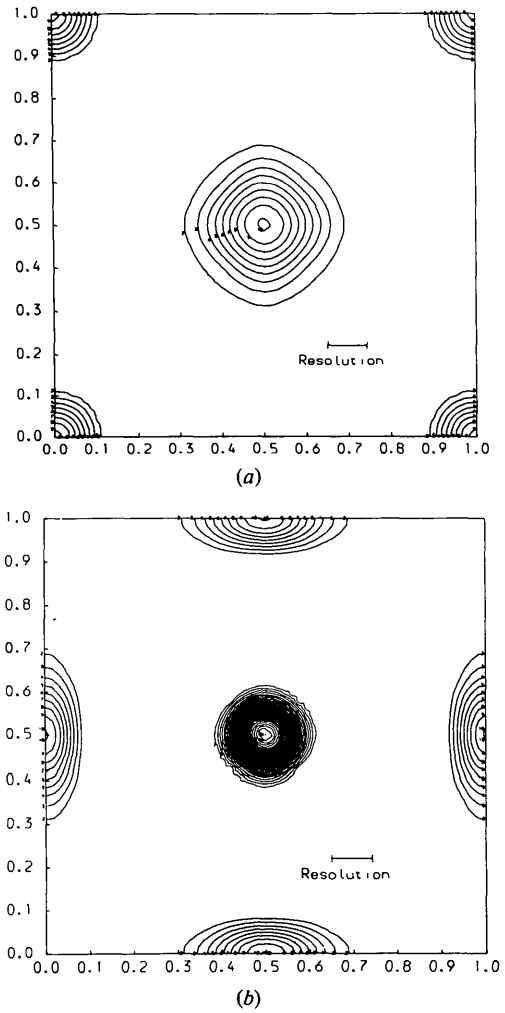

Fig. 6. Three-dimensional Fourier syntheses for cubic $CsPbCl_3$ at 325 K. Sections at $Z = 0{\cdot}0$ and $Z = 0{\cdot}5$ are shown in (*a*) and (*b*), respectively. Contour intervals of $0{\cdot}15$ (10^{-11} mm Å^{-3}).

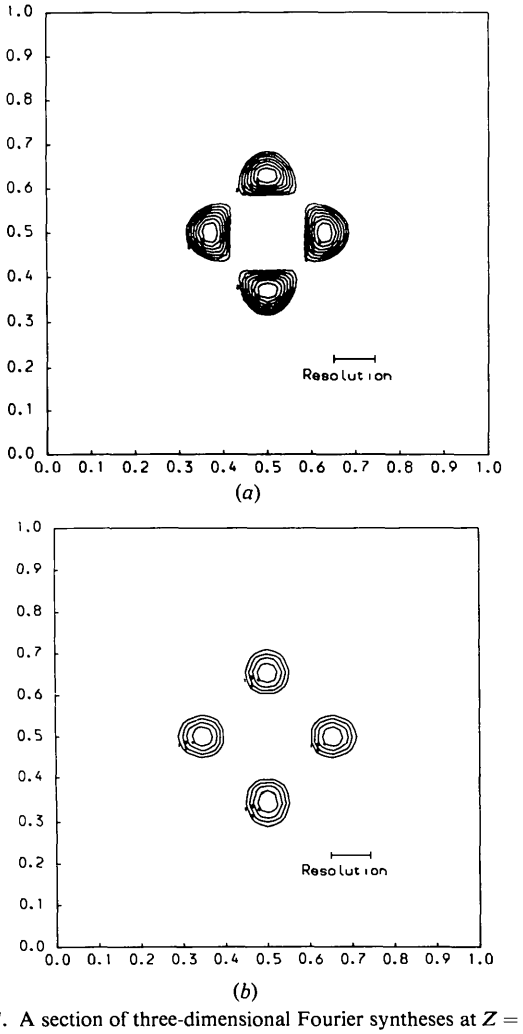

Fig. 7. A section of three-dimensional Fourier syntheses at $Z = 0{\cdot}0$ for cubic $CsPbCl_3$. Temperatures of 328 and 573 K are shown in (*a*) and (*b*) respectively. Contour integrals of $0{\cdot}003$ (10^{-11} mm Å^{-3}).

coefficient of the Cl atoms, D_{1122}(Cl), as expected from the least-squares analysis. The density of these peaks increases with decreasing temperature towards the phase transition, which is also consistent with the least-squares analysis as seen from Table 1. Therefore, the potential of the Cl atom has anisotropy in the (100) plane and is slightly shallow along the [010] and [001] directions.

It should be noticed, however, that these four peaks found from the difference Fourier map do not show any implication of the existence of a multiminimum potential. The condition for them to be a structural disorder would be a density maxima on a Fourier map, not on a difference Fourier map only. There is also no indication of disordering of the Cs atoms suggested previously by Møller (1959).

6. Discussion

The potential coefficients of atoms in a crystal including anharmonicity are usually determined from the analysis of the precise Q dependence of the integrated Bragg intensities obtained at one particular temperature. In this analysis, it is essential to decouple the higher-order term for Q in the temperature factor from the second-order term. However, this procedure is not always easy to do owing to the existence of correlation between the second- and the fourth-order potential coefficients in the least-squares refinement. In an early study of anharmonicity by Willis (1969), the anharmonic potential coefficients were determined from the temperature dependence of several Bragg intensities. In order to avoid such correlation problems, the method of analysing the temperature dependence of the B values has been employed by previous workers (Mair, Barnea, Cooper & Rouse, 1974; Harada, Suzuki & Hoshino, 1976). In the present study the analysis has been done in two stages, that is, the refinement of the B values at several temperatures and the refinement of potential coefficients on the basis of the temperature dependence of the B values. It is possible to extend the present method to refining the potential coefficients in a single stage directly from all the temperature-dependent Bragg intensity data.

Thermal vibrations in $CsPbCl_3$ and $CsPbBr_3$ were found to have very similar characteristics. The mean-square displacements of Cs atoms and halogen atoms are anomalously large. Besides, halogen atoms show extreme anisotropy. In spite of this they show much less temperature dependence throughout the whole range of temperature investigated, as shown in Figs. 1(*a*), (*c*) and 2(*a*), (*c*). Such characteristics of the thermal behaviour are attributed to the anharmonic potentials whose shape resembles the square-well type, as seen in Fig. 5 for both kinds of atoms. In contrast, the thermal vibrations of the Pb atoms are quite normal and are well described by harmonic potentials. It is very interesting to notice that the Cs and halogen atoms, which are located in anharmonic potentials in the cubic phase, displace their positions through the successive phase transitions.

In Figs. 1(*c*) and 2(*c*), it should also be noticed that near the phase transitions the temperature parameters for only the halogen atoms deviate from the temperature dependence which is expected on the basis of the anharmonic potentials determined by the present analysis. These deviations must be closely related to the fact that only halogen atoms are involved in the phase transitions from cubic to tetragonal structure.

References

BECKER, P. J. & COPPENS, P. (1974*a*). *Acta Cryst.* A**30**, 129–147.

BECKER, P. J. & COPPENS, P. (1974*b*). *Acta Cryst.* A**30**, 148–153.

CAVA, R. J., REIDINGER, F. & WUENSCH, B. J. (1977). *Solid State Commun.* **24**, 411–416.

COOPER, M. J. & ROUSE, K. D. (1970). *Acta Cryst.* A**26**, 214–223.

COOPER, M. J. & ROUSE, K. D. (1971). *Acta Cryst.* A**27**, 622–628.

DAWSON, B. (1967). *Proc. R. Soc. London Ser. A*, **298**, 255–263.

FUJII, Y., HOSHINO, S., YAMADA, Y. & SHIRANE, G. (1974). *Phys. Rev. B*, **9**, 4549–4559.

HARADA, J., SAKATA, M., HOSHINO, S. & HIROTSU, S. (1976). *J. Phys. Soc. Jpn*, **40**, 212–218.

HARADA, J., SUZUKI, H. & HOSHINO, S. (1976). *J. Phys. Soc. Jpn*, **41**, 1707–1715.

HIROTSU, S. (1971). *J. Phys. Soc. Jpn*, **31**, 551–560.

HIROTSU, S., HARADA, J., IIZUMI, M. & GESI, K. (1974). *J. Phys. Soc. Jpn*, **37**, 1393–1398.

JOHNSON, C. E. (1970). *Thermal Neutron Diffraction*, edited by B. T. M. WILLIS. Oxford Univ. Press.

MAIR, S. L., BARNEA, Z., COOPER, M. J. & ROUSE, K. D. (1974). *Acta Cryst.* A**30**, 806–813.

MATSUBARA, T. (1975*a*). *Prog. Theor. Phys.* **53**, 1210–1211.

MATSUBARA, T. (1975*b*). *J. Phys. Soc. Jpn*, **38**, 1076–1079.

MØLLER, C. K. (1959). *Mat.-Fys. Medd. K. Dan. Vidensk. Selsk.* **32**, No. 2.

NISHIWAKI, T., SAKATA, M. & HARADA, J. (1976). *J. Phys. Soc. Jpn*, **41**, 355–356.

OHTA, H., HARADA, J. & HIROTSU, S. (1973). *Solid State Commun.* **13**, 1969–1972.

OLBRYCHSKI, K. (1963). *Phys. Status Solidi*, **3**, 2143–2154.

SAKATA, M., COOPER, M. J., ROUSE, K. D. & WILLIS, B. T. M. (1978). *Acta Cryst.* A**34**, 336–341.

SAKATA, M., NISHIWAKI, T. & HARADA, J. (1979). *J. Phys. Soc. Jpn*, **47**, 232–233.

WILLIS, B. T. M. (1969). *Acta Cryst.* A**25**, 277–300.